NATIONAL ADVISORY COMMITTEE FOR AERONAUTICS

TECHNICAL NOTE 4192

THREE-DEGREE-OF-FREEDOM EVALUATION OF THE LONGITUDINAL TRANSFER FUNCTIONS OF A SUPERSONIC CANARD MISSILE CONFIGURATION INCLUDING CHANGES IN FORWARD SPEED

By Ernest C. Seaberg

Langley Aeronautical Laboratory
Langley Field, Va.

NACA

Washington

December 1957

M

NATIONAL ADVISORY COMMITTEE FOR AERONAUTICS

TECHNICAL NOTE 4192

THREE-DEGREE-OF-FREEDOM EVALUATION OF THE LONGITUDINAL TRANSFER FUNCTIONS OF A SUPERSONIC CANARD MISSILE CONFIGURATION INCLUDING CHANGES IN FORWARD SPEED[1]

By Ernest C. Seaberg

SUMMARY

A reevaluation of existing flight data obtained for a supersonic canard missile configuration of the boost-glide type has been made to determine derivatives not previously evaluated. These derivatives, together with those previously evaluated and published, have been utilized to determine some typical airframe frequency responses based on the three-degree-of-freedom longitudinal equations of motion.

For constant flight conditions, it is shown that besides the usual drag-coefficient variation, the velocity derivatives also vary with angle of attack or Mach number. The effect of angle-of-attack variation on the missile frequency responses which include the velocity derivatives in their solution is appreciable only in the low-frequency region of operation (below 10 radians/sec). When the velocity derivatives are neglected, this low-frequency variation with angle of attack is different. Some of these differences are pointed out in the results to indicate the significance of including the velocity derivatives in the solution for the transfer functions.

INTRODUCTION

Increased interest in the phugoid motion has been expressed from various sources, especially in connection with automatic airspeed or altitude control systems. The present study of the three-degree-of-freedom motion actually arose out of an investigation of an automatic altitude control system wherein the altitude-sensing instruments operate at a frequency considerably below the high-frequency airframe mode. In this situation, the influence of the low-frequency airframe dynamics on the overall stability of the system may prove to be important.

---

[1]Supersedes recently declassified NACA Research Memorandum L54C02 by Ernest C. Seaberg, 1954.

The main purpose of the present paper is to evaluate the longitudinal transfer functions of a supersonic canard missile by means of a reevaluation of the data obtained from previous flight tests of the missile in order to include the variation of drag coefficient with angle of attack and the variation of force and moment coefficients with velocity in the solution of the three-degree-of-freedom equations of motion. The variation of these additional derivatives with Mach number is presented herein for several values of angle of attack. The longitudinal transfer functions in the form of frequency-response plots for several flight conditions are also given.

In reference 1, the effect of a fourth degree of freedom (namely, variation of height) on the longitudinal motion of full-scale aircraft is discussed. Although this additional degree of freedom may influence the longitudinal motion of missiles to some extent, the study of this effect was not included in the present investigation. The present investigation is mainly concerned with the additional effects of variation of force and moment coefficients with velocity, as compared with previous three-degree-of-freedom studies (ref. 2, for example) wherein these effects were not considered.

SYMBOLS

θ	pitch-attitude angle, radians
α	angle of attack, radians unless otherwise indicated
β	angle of sideslip, radians
γ	flight-path angle, radians
ζ	critical damping ratio
δ	canard elevator deflection, radians
m	mass, 5.05 slugs
W	weight, 163 pounds
S	wing area, 4.1 sq ft
Y	stability axis which passes through center of gravity and is perpendicular to vertical plane of symmetry
I_Y	moment of inertia about Y-axis, 31.3 slug-ft^2

$\bar{c}$	mean aerodynamic chord, 1.776 ft
x_{sm}	static margin, ft
M	Mach number
V	velocity, ft/sec
$u = \frac{\Delta V}{V}$	
q	dynamic pressure, lb/sq ft
t	time, sec
D	differential operator, d/dt
G(D)	transfer function expressed as a linear function of D
$\lvert G(D) \rvert$	amplitude or magnitude of G(D)
db	decibels, $20 \log_{10} \lvert G(D) \rvert$
ϕ	phase angle of G(D), deg
ω	angular frequency, radians/sec
ω_n	undamped natural frequency, radians/sec
C_L	lift coefficient, Lift/qS
C_D	drag coefficient, Drag/qS
C_m	pitching-moment coefficient, $\frac{\text{Pitching moment}}{qS\bar{c}}$

$C_{L_\alpha} = \partial C_L / \partial \alpha$

$C_{m_\delta} = \partial C_m / \partial \delta$

$C_{m_\alpha} = \partial C_m / \partial \alpha$

$C_{m_{\dot{\alpha}}} = \partial C_m \Big/ \partial \frac{\dot{\alpha}\bar{c}}{2V}$

$C_{m_q} = \partial C_m / \partial \frac{\dot{\theta}\bar{c}}{2V}$

$C_{D_\alpha} = \partial C_D / \partial \alpha$

$C_{D_u} = \partial C_D / \partial u$

$C_{L_u} = \partial C_L / \partial u$

$C_{m_u} = \partial C_m / \partial u$

Subscripts:

p	phugoid
o	equilibrium value

Dot over a symbol denotes derivative with respect to time.

METHODS AND APPARATUS

Equations of Motion

The three-degree-of-freedom longitudinal equations of motion, assuming small disturbances from steady symmetric horizontal flight, are:

$$\left(\frac{W}{qS}\cos\gamma_o\right)\theta + \left(C_{D_\alpha} - \frac{W}{qS}\cos\gamma_o\right)\alpha + \left(\frac{mV}{qS}D + C_{D_u} + 2C_D\right)u = 0$$

$$\left(\frac{mV}{qS}D - \frac{W}{qS}\sin\gamma_o\right)\theta - \left(\frac{mV}{qS}D + C_{L_\alpha} - \frac{W}{qS}\sin\gamma_o\right)\alpha - \left(C_{L_u} + 2C_L\right)u = 0$$

$$\left(\frac{I_Y}{qS\bar{c}}D^2 - \frac{\bar{c}}{2V}C_{m_q}D\right)\theta - \left(C_{m_\alpha} + \frac{\bar{c}}{2V}C_{m_{\dot{\alpha}}}D\right)\alpha - C_{m_u}u = C_{m_\delta}\delta$$

Various derivations and forms of these equations can be found elsewhere. (See, for example, refs. 2 to 7.) In these references various notations are used; in some more terms are included than in the present report, and in others terms which are included herein are neglected. The equations presented here, however, satisfactorily define the motion of the missile under consideration with the assumption of small disturbances. The notation used is based on the stability system of axis and parallels the more widely used two-degree-of-freedom equations. (See ref. 8.)

Flight-Data Presentation

Airframe.- The airframe on which this analysis is based is an all-metal research model of the canard missile type. A photograph and a sketch of the actual model used for previous flight testing is shown in figure 1. References 9 and 10 give more complete descriptions of this model and present the flight data in the form of aerodynamic stability derivatives used in previous two-degree-of-freedom analyses. In reference 8, values of these derivatives are tabulated for typical flight conditions. The additional derivatives necessary for the three-degree-of-freedom study presented herein were obtained from a reevaluation of the flight data presented in references 9 and 10 and from the results of other flight testing not previously published.

C_{D_α}.- The derivative C_{D_α} was evaluated from the results of flight tests not previously reported, wherein the model was roll stabilized and pulsed in pitch and yaw, and the values of C_D based on total drag along the velocity vector were plotted against total angle of attack $\sqrt{\alpha^2 + \beta^2}$. Sufficient curves were obtained to cover a Mach number range of approximately 1 to 1.7. The slopes of tangents to curves obtained in the foregoing manner were then measured to determine the C_{D_α} data presented herein. Since a symmetrical cruciform missile is being dealt with, a value of C_{D_α} based on total drag and total angle of attack is equivalent to one based on measurements in the pitch plane alone and is valid for use in the longitudinal equations of motion.

C_{D_u}, C_{L_u}, and C_{m_u}.- In this case the variations of the coefficients C_D, C_L, and C_m with velocity were first obtained. Sufficient data were available to cover a velocity range of approximately 1,000 to 2,000 feet per second, assuming standard sea-level conditions. The angle-of-attack range covered was as high as 10° or 12°. The slopes of tangents to these curves were then measured to obtain the nondimensional derivatives such as $C_{D_u} = \partial C_D/\partial u$ which are presented herein as functions of Mach number for constant values of angle of attack.

Frequency Responses

A solution of the equations of motion to obtain the transfer functions can only be obtained by assuming an equilibrium Mach number and then selecting values of C_{D_α}, C_{D_u}, C_{L_u}, and C_{m_u} for the trim angle-of-attack value under consideration. Solutions based on the foregoing assumptions are presented in the results as frequency-response plots of the transfer functions. A particular transfer function, for instance θ/δ, is obtained by expansion of its determinant to yield the function

$$\frac{\theta}{\delta} = G(D)$$

The frequency response of this function is then plotted through the use of templates as described in chapter 8 of reference 11.

RESULTS AND DISCUSSION

Derivatives

C_{D_α}.- Plots of C_{D_α} against Mach number for constant values of α are shown in figure 2. For a constant Mach number, this derivative exhibits a decided increase with increasing α and for the lower values of α, C_{D_α} decreases to a steady value with increasing M. The decrease with increasing M is more apparent at the higher values of α for the Mach number range shown.

C_{D_u}, C_{L_u}, and C_{m_u}.- The velocity derivatives C_{D_u}, C_{L_u}, and C_{m_u} are plotted against M for constant values of α in figure 3. The trends exhibited by C_{D_u} and C_{L_u} (figs. 3(a) and (b)) are somewhat similar in that at subsonic Mach numbers the curves show positive values which decrease to zero at approximately M = 1.03 and then increase negatively to maximum values between M = 1.2 and M = 1.35. From this point, a more gradual rise back toward zero is noted for C_{L_u} than for C_{D_u}.

Curves of C_{m_u} against M for constant values of α are shown in figure 3(c). From these curves it is seen that C_{m_u} is negative at subsonic Mach numbers, and is zero for all values of α at approximately M = 1.03. The values of C_{m_u} then increase to maximum positive values at M = 1.55 approximately, after which a decrease with increasing M is shown. The uniform spread in the curves of this figure indicates that

the variation of this derivative with α for a constant Mach number is fairly linear.

C_D and C_L.- The values of C_D and C_L used in computing the transfer functions presented herein are shown in table I. Except for the zero-lift drag coefficient, the C_D values have not been previously published. The C_L values are presented for completeness although they are indirectly available in published form elsewhere.

Frequency Responses

Typical missile frequency responses obtained from a solution of the three-degree-of-freedom equations of motion are shown in figures 4 and 5. These responses are based on standard sea-level conditions at $M = 1.6$ with a missile static margin of $0.29\bar{4}c$. The responses θ/δ, α/δ, and u/δ were obtained directly from a solution of the equations of motion as given herein previously, whereas the substitution $\gamma = \theta - \alpha$ was employed to obtain the γ/δ responses (figs. 4(d) and 5(d)). For each of the variables, the amplitude and phase response obtained for trim angle-of-attack values of 0°, 4°, and 10° are shown. This implies that the derivatives C_{D_α}, C_{D_u}, C_{L_u}, and C_{m_u} and the values of C_D and C_L correspond to the trim angle-of-attack value under consideration for each solution, despite the variations with α shown in figures 2 and 3 and table I.

Effect of including velocity derivatives.- The frequency responses obtained at $M = 1.6$ including the effect of velocity derivatives are shown in figure 4. Phase shifts as the frequency approaches zero and changes in static sensitivity are shown for the trim angle-of-attack values investigated. In figures 4(a) and 4(d), for example, as the frequency decreases, the phase curves for θ/δ and γ/δ are shown to tend toward -90°, 0°, and 180° as the trim angle of attack is changed from 0° to 4° to 10°, respectively. At a trim α of 0° the solution is similar to that obtained for two degrees of freedom with an integration effectively present because of the zero lift force. At $\alpha = 4^\circ$ the characteristic equation (denominator of transfer function) is of the biquadratic form

$$\left(D^2 + 2\zeta_p\omega_{n_p} D + \omega_{n_p}{}^2\right)\left(D^2 + 2\zeta\omega_n D + \omega_n{}^2\right)$$

with a positive static sensitivity yielding a zero initial phase relation. For $\alpha = 10^\circ$, however, the numerators of the transfer functions θ/δ and

γ/δ contain a negative linear term yielding a negative static sensitivity and causing the 180° initial phase shift.

For angular frequencies above 10 radians/sec, with the exception of u/δ (fig. 4(c)), changing the trim angle of attack has only a slight effect on the frequency response obtained, since for this particular missile the static stability derivatives have previously been shown to be fairly linear. The effect of changing the trim angle of attack would therefore be considered negligible in control-system applications where the controlling elements are designed to operate at a frequency in excess of the high-frequency airframe mode. The reasoning in this case is that the overall transient behavior of a control system in combination with the airframe would be essentially the same regardless of the trim α, since the contribution of the airframe would not change appreciably with angle of attack in the region of the control-system operating frequency.

The curves presented in figure 4 also indicate that the phugoid mode is more heavily damped than the high-frequency mode. The values of phugoid critical damping ratio given in the first part of table II are 0.84 at $\alpha = 4^\circ$ and 1.96 at $\alpha = 10^\circ$, compared with values of $\zeta \approx 0.15$ for the high-frequency mode. The large value of ζ_p at $\alpha = 10^\circ$ indicates that the phugoid mode in this case is nonoscillatory, actually consisting of two aperiodic modes. This large value of ζ_p can be attributed to the large drag obtained for supersonic flight at this angle of attack. The values of undamped natural frequency given in table II where the velocity derivatives are included are approximately 0.15 radian/sec for the low-frequency mode and 26 radians/sec for the high-frequency mode. The values of the static sensitivity (actual static ratios) of the various transfer functions are also given in table II. With the exception of α/δ, the static sensitivities are infinite at $\alpha = 0^\circ$ and finite when a value is assumed for α. In any case the absolute values of the θ/δ and γ/δ static sensitivities are fairly large (for instance, the static value of θ/δ is 29.1 at $\alpha = 4^\circ$ and -14.8 at $\alpha = 10^\circ$ and the infinite value at $\alpha = 0^\circ$ is, of course, due to the previously mentioned integration.) These large or negative values of static sensitivity, however, may not be too significant since, with the assumption of small perturbations, large steady-state values would only be applicable for extremely small values of δ.

Effect of neglecting velocity derivatives.- The frequency responses shown in figure 5 are comparable to those shown in figure 4 except that in figure 5 the velocity derivatives are neglected (that is, $C_{D_u} = C_{L_u} = C_{m_u} = 0$). The characteristic-equation and static-sensitivity values for this case are also summarized in table II. Except for variations in static sensitivity, table II, however, does not reveal anything very significant concerning the effect of the velocity derivatives. Referring again to figures 4 and 5, the variations between the responses

shown in figure 5 and the corresponding responses shown in figure 4 are mainly in the low-frequency region. A close comparison of the θ/δ responses shown in figures 4(a) and 5(a) reveals some differences in the shapes of the amplitude and phase responses in the low-frequency region. The nature of the responses, however, makes the effect of including or neglecting the velocity derivatives more readily apparent in a comparison of the α/δ responses (figs. 4(b) and 5(b)). In figure 5(b) it is shown that changing the angle of attack has very little effect on the response. This result arises from the mathematics of the transfer function, since the numerator terms practically cancel the phugoid quadratic regardless of the angle of attack. However, when the velocity derivatives are included, as in figure 4(b), this is not the case. Here the amplitude-ratio curves exhibit noticeable change in static sensitivity when a value of α is assumed and the phase curves show leading characteristics in the low-frequency region. The leading characteristics arise from the fact that the numerator terms break at lower frequencies than the phugoid mode of motion.

Effect of Mach number change.- The data presented in table III are comparable in every respect to those presented in table II except that the values presented are based on a Mach number of 1.2. Variations between the corresponding values of the two tables can be noted. Perhaps the most significant of these is the value of the phugoid critical damping ratio at $\alpha = 4^\circ$ for the case where the velocity derivatives are included. In this case $\zeta_p = 0.374$ and the low value can be attributed to a high value of C_{D_u}. Reference to figure 3(a) shows that for the $\alpha = 4^\circ$ curve, $C_{D_u} \approx -0.07$ or very nearly its negative maximum for this angle of attack. The absolute value of C_{D_u} for this case is actually greater than C_D. (See table I.) Although the curves are not shown, the frequency responses for $M = 1.2$ and $\alpha = 4^\circ$ would exhibit more peaking of the amplitude ratio and more rapid phase changing in the region of the phugoid undamped natural frequency (0.115 radian/sec) than any of those shown for $M = 1.6$ because of the lower critical damping ratio.

Three-Degree-of-Freedom Approach to Future Automatic-Control Studies

Since the frequency response obtained with constant flight conditions is shown to vary with the trim angle of attack, particularly in the low-frequency region, the analysis of automatic-control systems which operate at low frequencies – for example, altitude or airspeed controls – should define the airframe on the basis of three degrees of freedom. The transfer-function approach may be essential in preliminary analysis employing linear servomechanism theory. Therefore, in analyzing the altitude control, for example, depending on the angle-of-attack range

anticipated, three or more airframe transfer functions should be computed for each case with flight conditions and all other system components held constant. Then, depending on the component gain adjustments, it is probable that the stability of the system can be adequately predicted if no instabilities arise, regardless of the trim angle of attack on which the airframe transfer function happens to be based. It is obvious that more than one transient solution will be obtained for an equilibrium Mach number under these conditions. Although it can only be surmised at this time, it is anticipated that the actual transient behavior of the entire control system will be within the range of the solutions obtained for a number of different trim values of angle of attack. In order to obtain the unique solution for a constant set of flight conditions, the airframe can be represented by equations of motion, wherein some of the coefficients are represented as functions of the variable α. The airframe defined in this manner is nonlinear but can be combined with the rest of the automatic-control-system components through the use of an analog computer (REAC, for example) to obtain the unique solution. This, however, is a lengthy process; nevertheless, it may eventually be necessary to determine the validity of the previous surmise.

CONCLUDING REMARKS

The additional derivatives necessary for solution of the three-degree-of-freedom longitudinal equations of motion, namely, the velocity derivatives and the slope of the curve of drag coefficient against angle of attack, are shown to vary with angle of attack. This variation affects the missile frequency responses mainly in the low-frequency region. Therefore, in the analysis of a control system which operates at a high frequency, the contribution of an airframe with linear static characteristics would be essentially the same for all angle-of-attack values.

A comparison of the frequency responses obtained when the velocity derivatives are included with those obtained when the velocity derivatives are neglected reveals variations in the low-frequency region. The angle-of-attack frequency response, for example, exhibits noticeable changes in static sensitivity and more pronounced leading phase characteristics when the velocity derivatives are included than when the velocity derivatives are neglected.

The critical damping ratio was found to be higher for the phugoid mode of motion than for the high-frequency airframe mode. For low supersonic Mach numbers, however, where the derivative of the drag coefficient with respect to velocity is near its negative peak, the phugoid critical damping ratio may assume a fairly low value.

For the supersonic canard missile used in this investigation, the velocity derivatives reverse sign in the transonic region and have their maximum absolute values for supersonic flight in the range of Mach number from 1.2 to 1.55. Their absolute values then decrease with further increase in Mach number.

In applying three-degree-of-freedom transfer functions to automatic-control-system analysis, more than one airframe transfer function should be investigated for an equilibrium Mach number and constant automatic-control component gains. Then it is probable that the stability of the overall system can be adequately predicted if no instabilities arise, regardless of the trim angle of attack on which the airframe transfer function happens to be based. It is further surmised that the unique transient solution for an equilibrium Mach number will be within the range of the solutions based on airframe transfer functions covering a range of assumed trim angle-of-attack values.

Langley Aeronautical Laboratory,
National Advisory Committee for Aeronautics,
Langley Field, Va., February 16, 1954.

REFERENCES

1. Neumark, S.: Dynamic Longitudinal Stability in Level Flight, Including the Effects of Compressibility and Variations of Atmospheric Characteristics With Height. Rep. No. Aero.2265, British R.A.E., May 1948.

2. Cohen, Doris: Analytical Investigation of the Stability of an F8F Dropping Model With Automatic Stabilization. NACA WR L-780, 1945. (Formerly NACA MR L5L03.)

3. Zimmerman, Charles H.: An Analysis of Longitudinal Stability in Power-Off Flight With Charts for Use in Design. NACA Rep. 521, 1935.

4. Greenberg, Harry: Frequency-Response Method for Determination of Dynamic Stability Characteristics of Airplanes With Automatic Controls. NACA Rep. 882, 1947. (Supersedes NACA TN 1229.)

5. Mokrzycki, G. A.: Application of the Laplace Transformation to the Solution of the Lateral and Longitudinal Stability Equations. NACA TN 2002, 1950.

6. Abzug, M. J.: Equations of Airplane Motion, Including Power and Compressibility Effects. Sperry Rep. No. 5232-3196, Sperry Gyroscope Co., Nov. 1950.

7. Anon.: Fundamentals of Design of Piloted Aircraft Flight Control Systems. Vol. II - Dynamics of the Airframe. Rep. AE-61-4, Bur. Aero., Feb. 1953.

8. Seaberg, Ernest C., and Smith, Earl F.: Theoretical Investigation of an Automatic Control System With Primary Sensitivity to Normal Accelerations As Used To Control a Supersonic Canard Missile Configuration. NACA RM L51D23, 1951.

9. Gardiner, Robert A., and Zarovsky, Jacob: Rocket-Powered Flight Test of a Roll-Stabilized Supersonic Missile Configuration. NACA RM L9K01a, 1950.

10. Zarovsky, Jacob, and Gardiner, Robert A.: Flight Investigation of a Roll-Stabilized Missile Configuration at Varying Angles of Attack at Mach Numbers Between 0.8 and 1.79. NACA TN 3915, 1957. (Supersedes NACA RM L50H21.)

11. Brown, Gordon S., and Campbell, Donald P.: Principles of Servomechanisms. John Wiley & Sons, Inc., c.1948.

TABLE I

C_D AND C_L VALUES

α, deg	C_D for —		C_L for —	
	M = 1.2	M = 1.6	M = 1.2	M = 1.6
0	0.05	0.04	0	0
4	.063	.051	.211	.182
10	.152	.128	.527	.456

TABLE II

SUMMARY OF TRANSFER-FUNCTION CHARACTERISTIC EQUATIONS AND STATIC SENSITIVITIES

[M = 1.6; sea level; $x_{sm} = 0.294\bar{c}$]

Characteristic Equation

Including velocity derivatives				
α, deg	ω_{n_p}, radians/sec	ζ_p	ω_n, radians/sec	ζ
0	-----	----	26.25	0.152
4	0.132	0.84	26.2	.152
10	.207	1.96	26.1	.145
Neglecting velocity derivatives				
0	----	----	26.25	.152
4	.105	.83	26.2	.152
10	.166	1.31	26.2	.152

Static Sensitivities

Including velocity derivatives				
α, deg	θ/δ	α/δ	u/δ, per radian	γ/δ
0	∞	0.9	∞	∞
4	29.1	.5	-4.2	28.6
10	-14.8	.5	-1.7	-15.3
Neglecting velocity derivatives				
0	∞	.9	∞	∞
4	41.8	.9	-6.7	40.9
10	-28.9	.9	-2.6	-29.8

TABLE III

SUMMARY OF TRANSFER FUNCTION CHARACTERISTIC

EQUATIONS AND STATIC SENSITIVITIES

[M = 1.2; sea level; $x_{sm} = 0.339\bar{c}$]

Characteristic Equation

Including velocity derivatives				
α, deg	ω_{n_p}, radians/sec	ζ_p	ω_n, radians/sec	ζ
0	-----	-----	22.8	0.146
4	0.115	0.374	22.8	.146
10	.182	1.23	22.7	.142
Neglecting velocity derivatives				
0	-----	-----	22.8	.14
4	.114	.711	22.8	.146
10	.179	1.07	22.7	.146

Static Sensitivities

Including velocity derivatives				
α, deg	θ/δ	α/δ	u/δ, per radian	γ/δ
0	∞	.8	∞	∞
4	8	.6	-5.6	7.4
10	-11	.5	-2.2	-11.5
Neglecting velocity derivatives				
0	∞	.8	∞	∞
4	26.6	.8	-5.7	25.8
10	-16	.8	-2.3	-16.8

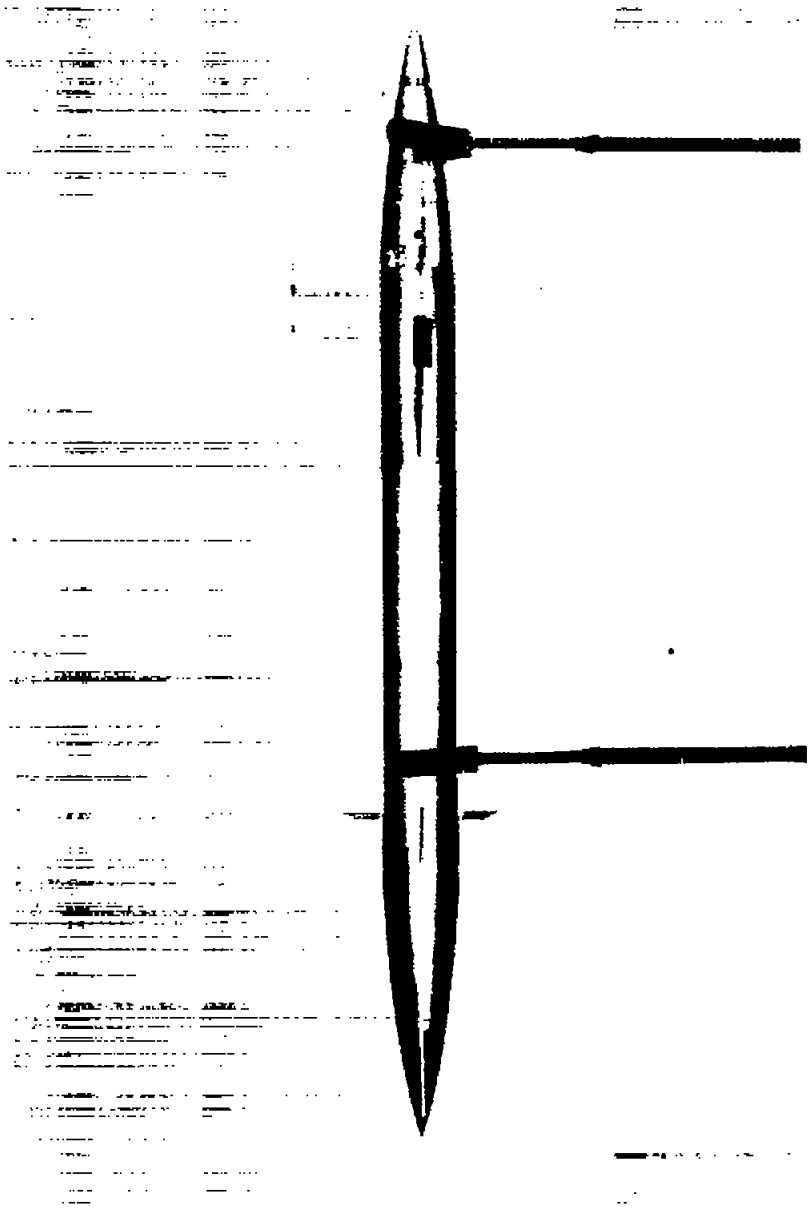

L-63726.1

(a) Photograph of model.

Figure 1.- Supersonic research model.

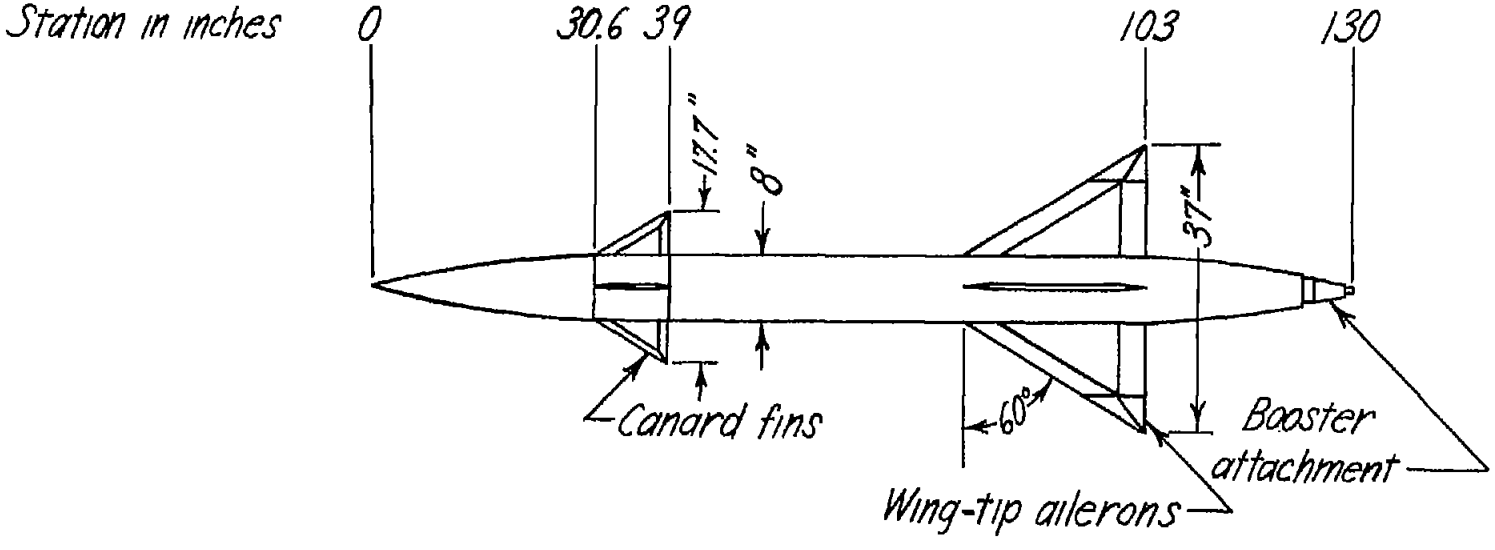

(b) Plan-view sketch of model.

Figure 1.- Concluded.

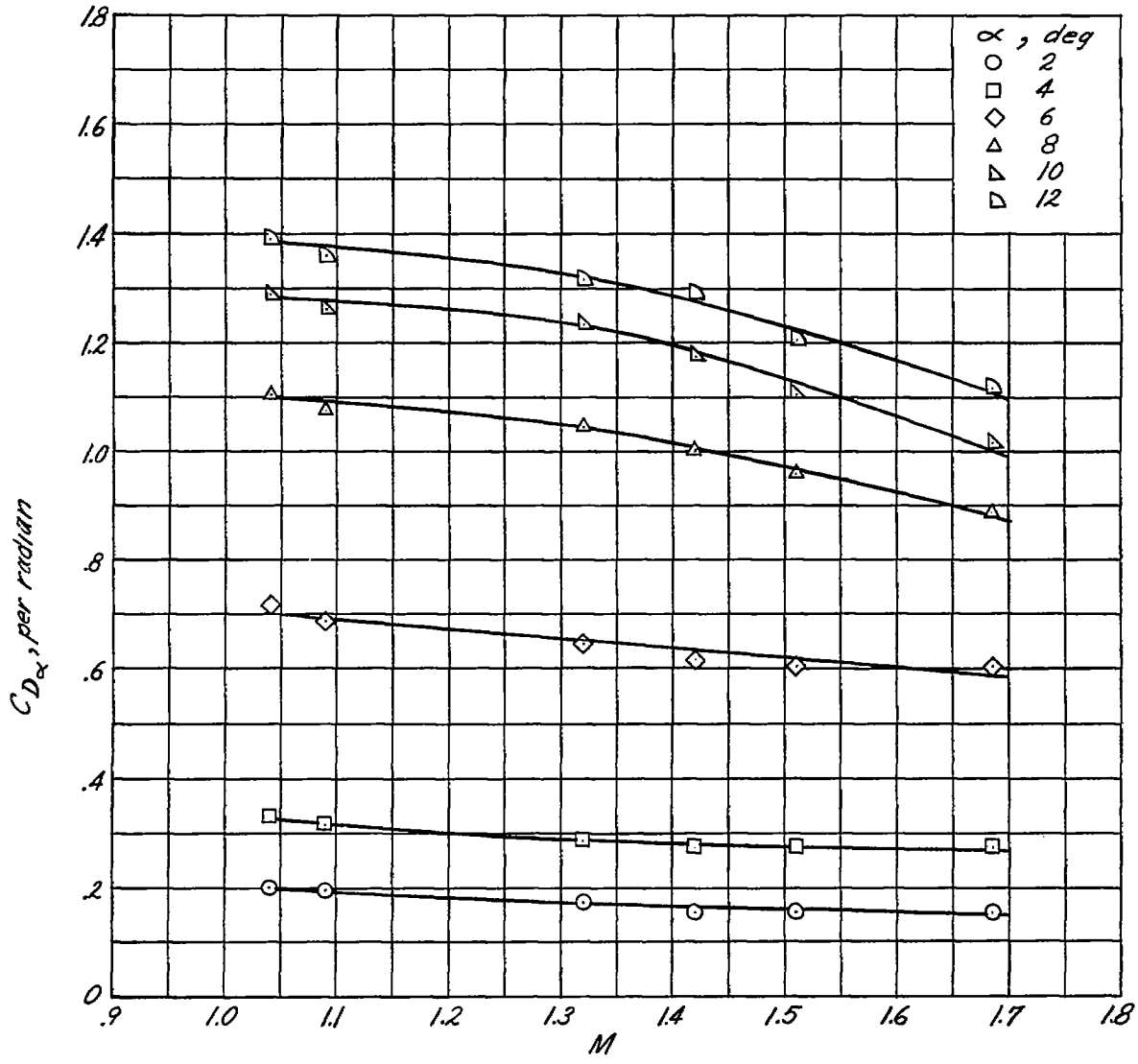

Figure 2.- Variation of C_{D_α} with Mach number for constant values of angle of attack.

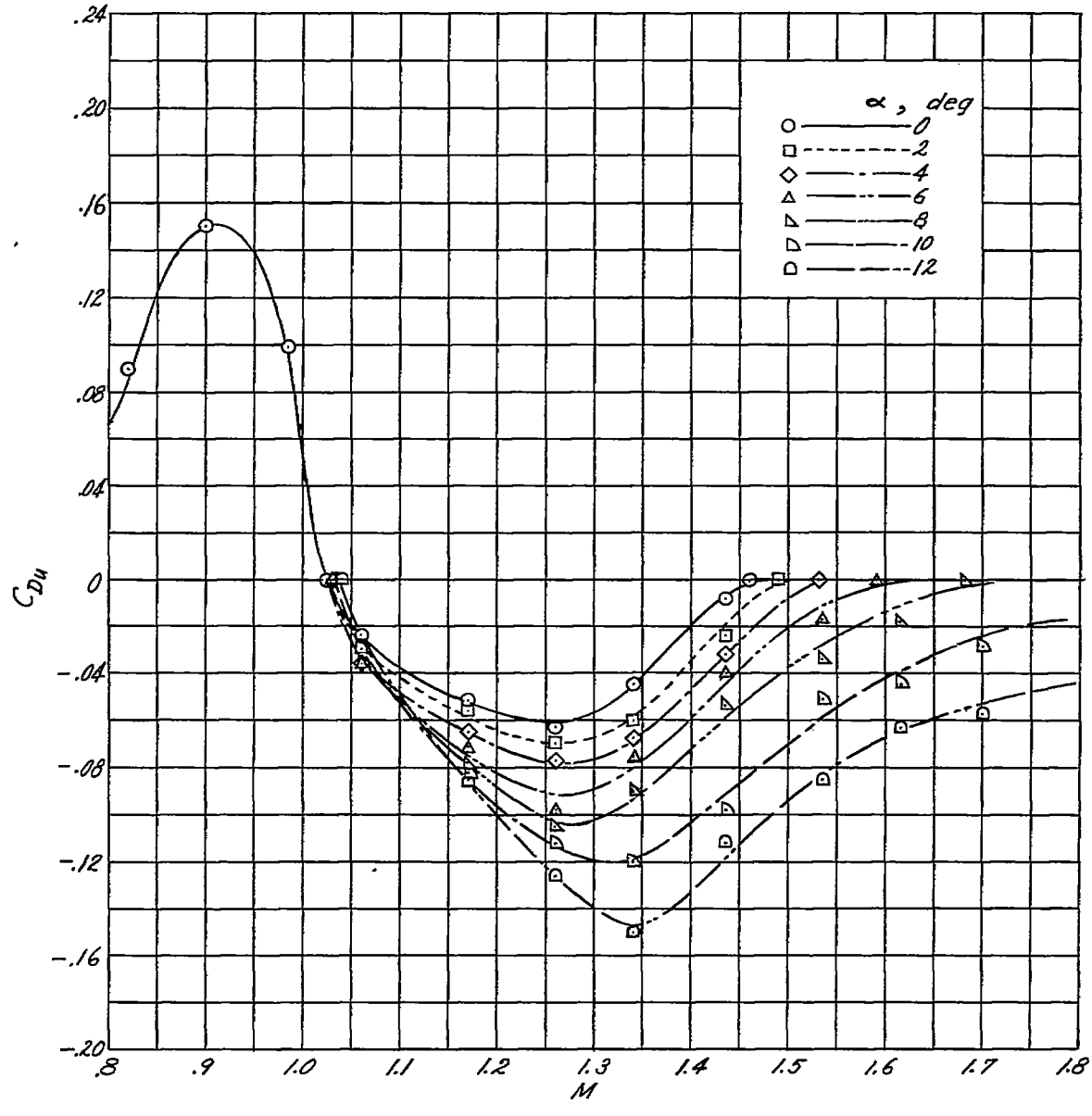

(a) C_{D_u}.

Figure 3.- Variation of velocity derivatives with Mach number for constant values of angle of attack.

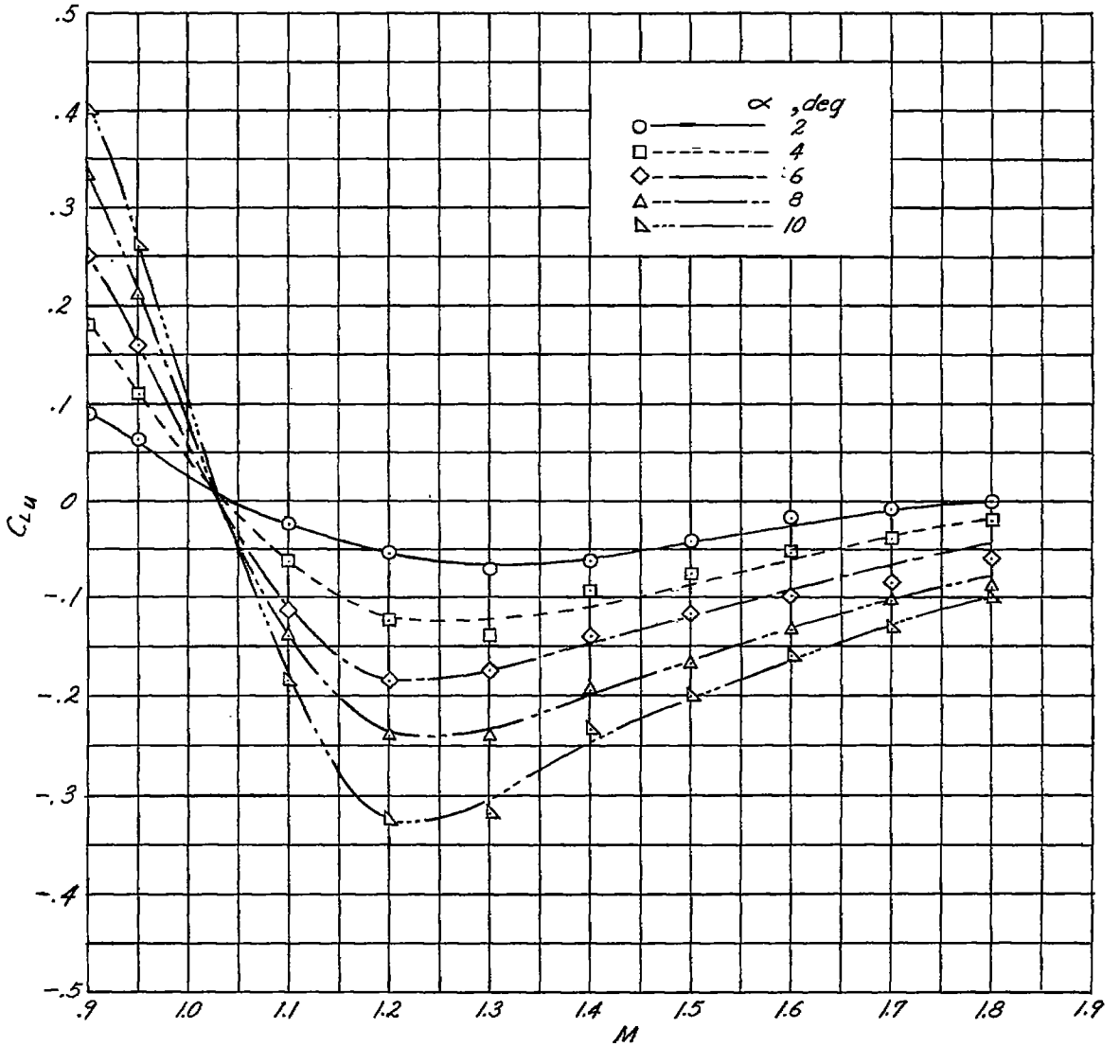

(b) C_{L_u}.

Figure 3.- Continued.

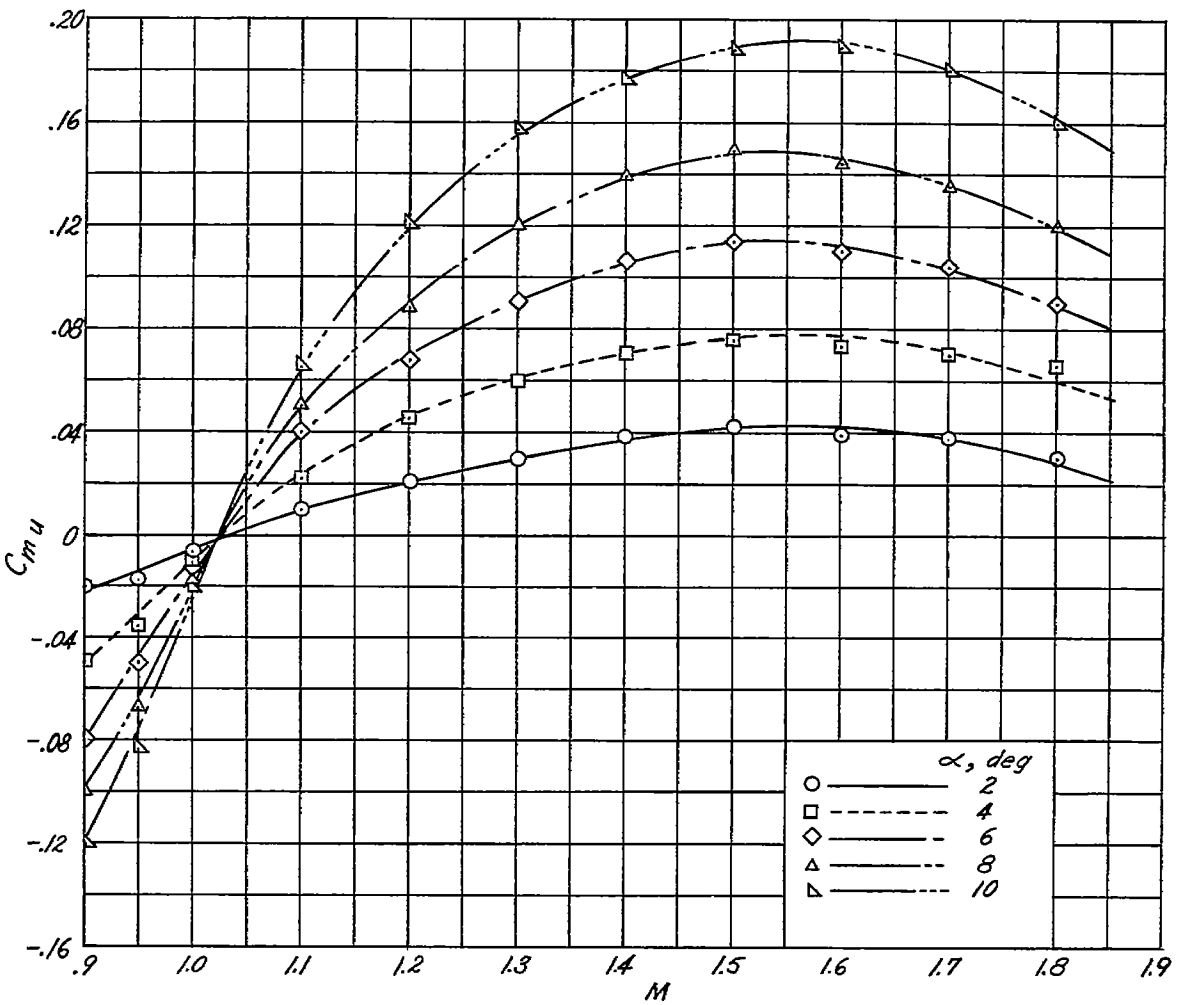

(c) C_{m_u}.

Figure 3.- Concluded.

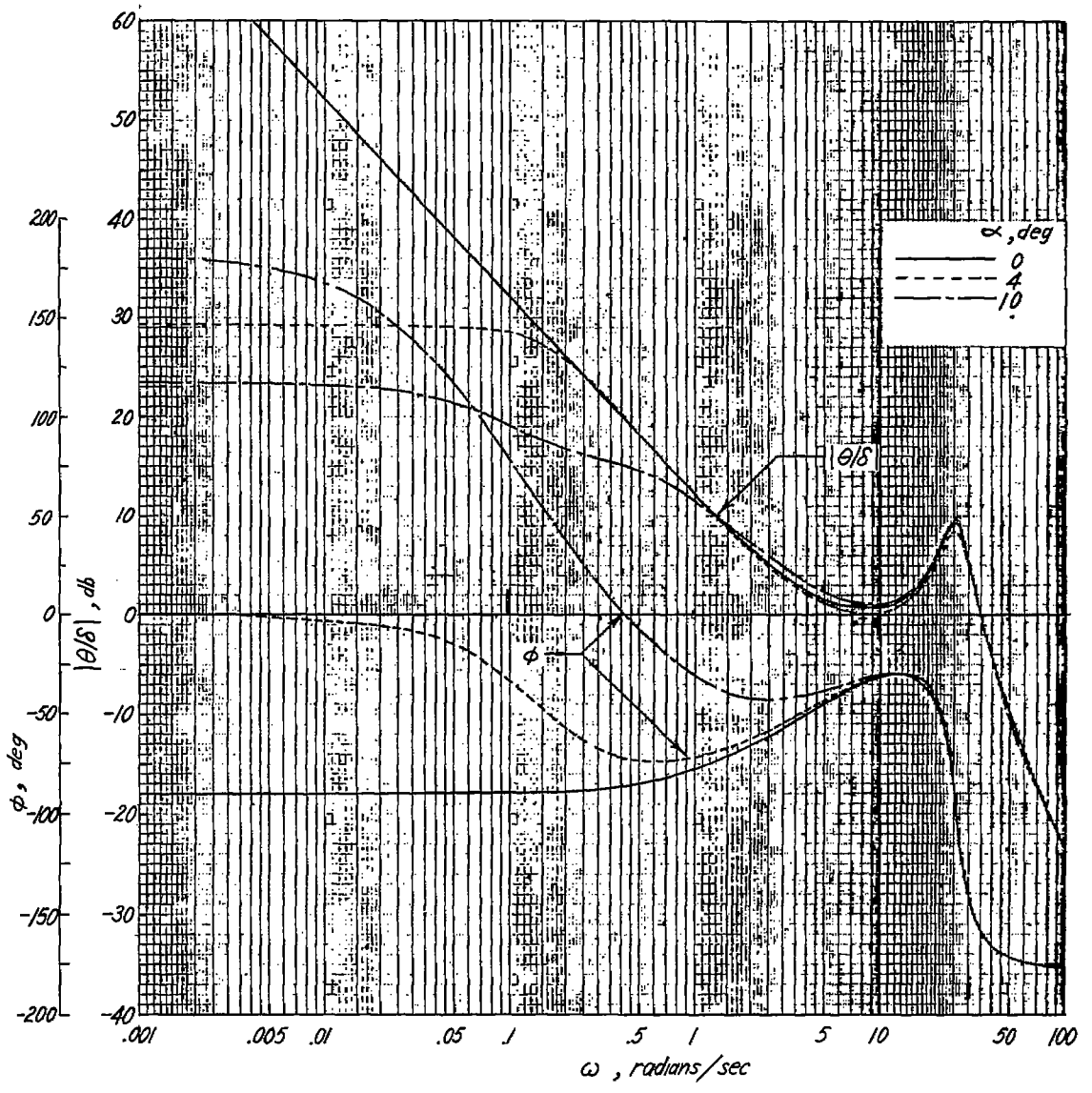

(a) θ/δ.

Figure 4.- Three-degree-of-freedom longitudinal frequency responses including effect of velocity derivatives for three values of trim α. These responses are based on standard sea-level conditions at $M = 1.6$ with $x_{sm} = 0.294\bar{c}$.

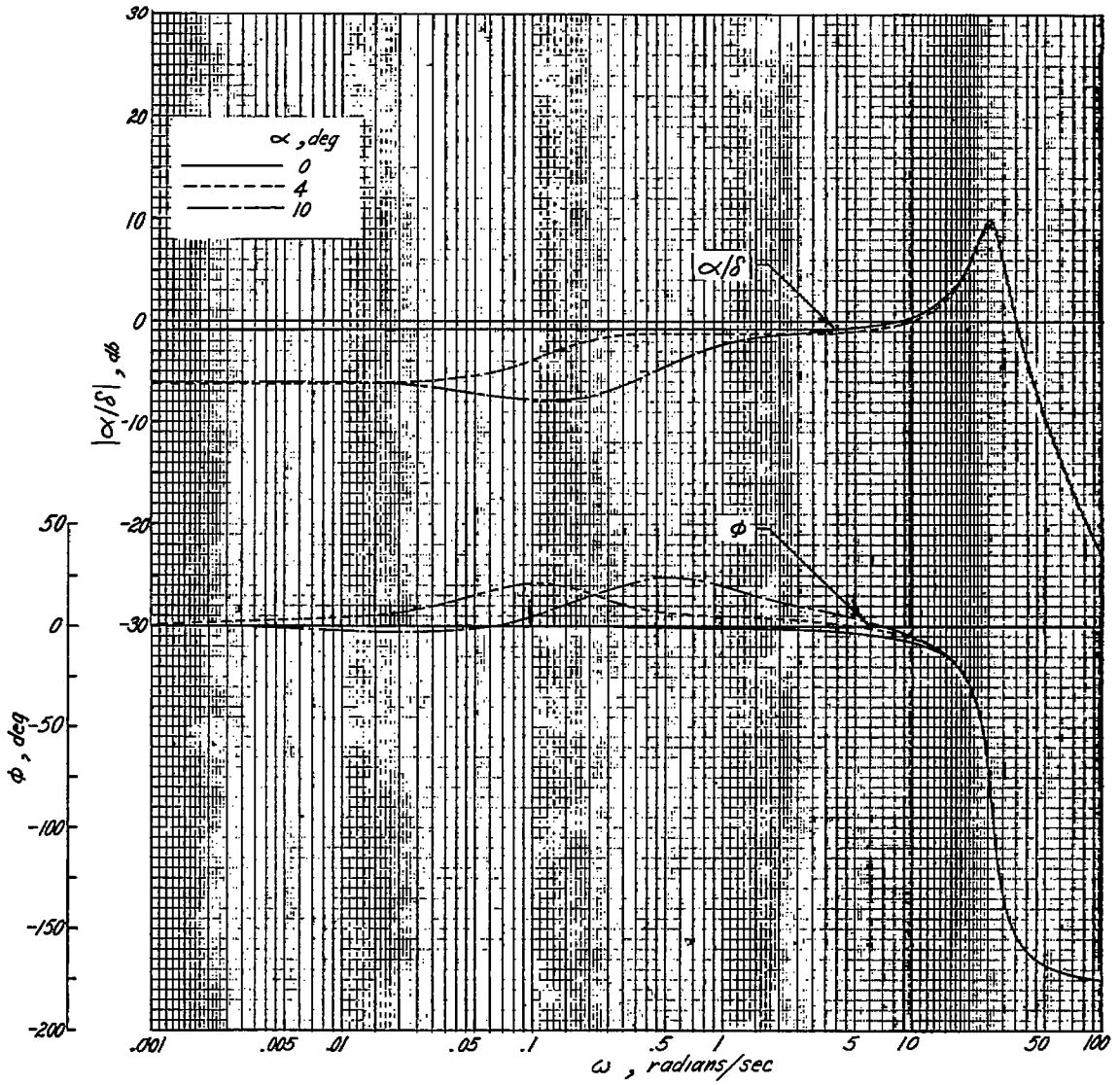

(b) α/δ.

Figure 4.- Continued.

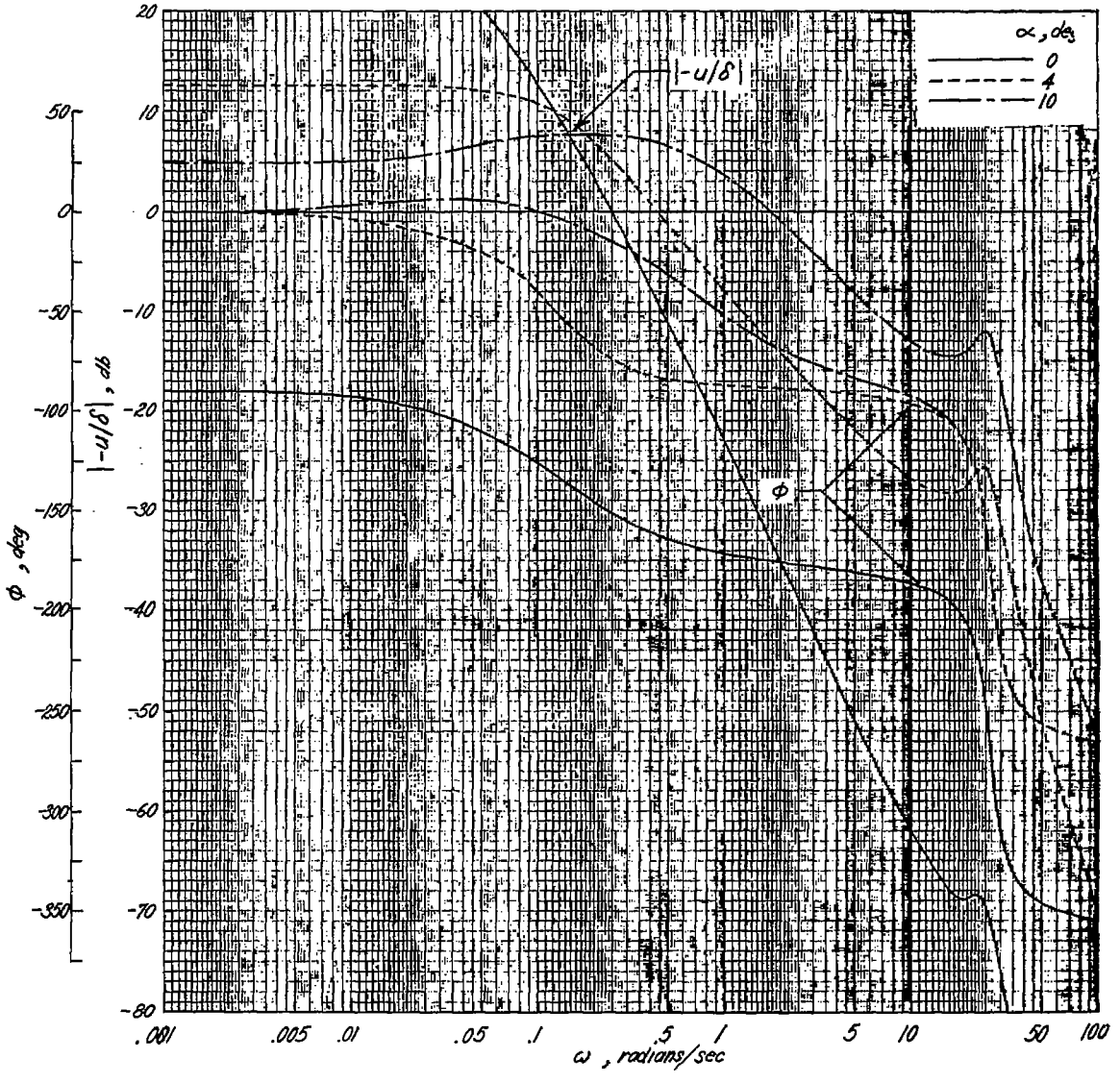

(c) $-u/\delta$.

Figure 4.- Continued.

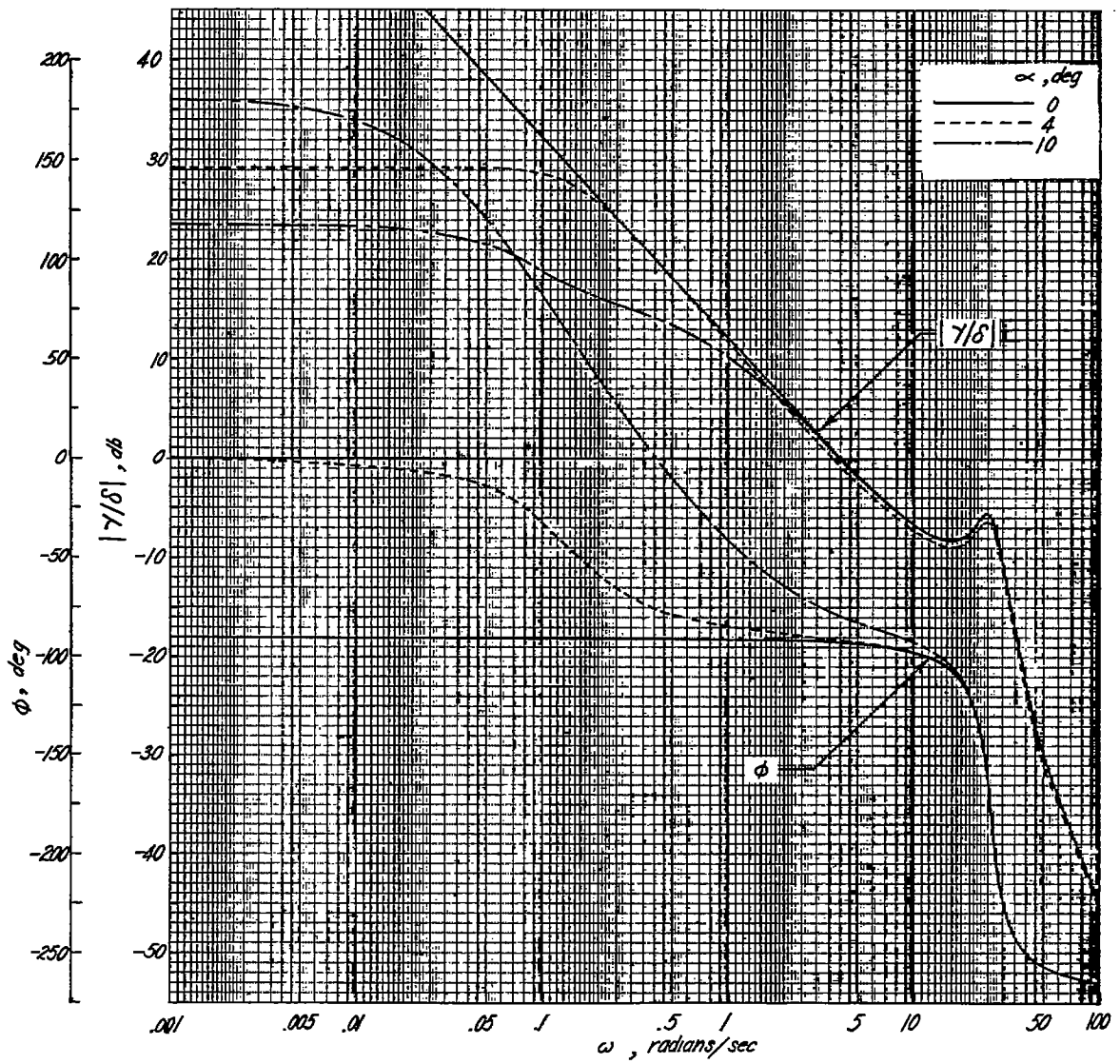

(d) γ/δ.

Figure 4.- Concluded.

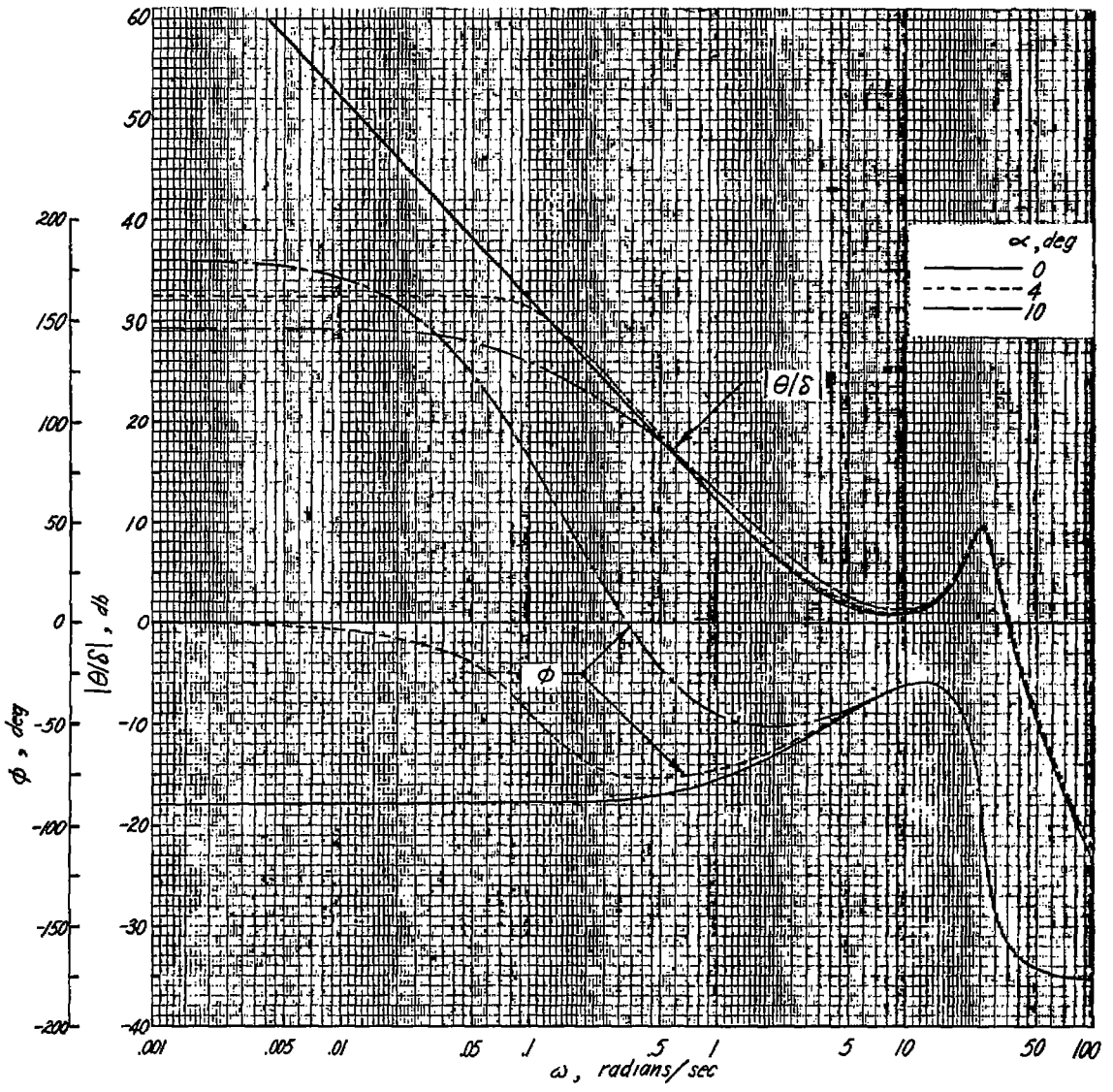

(a) θ/δ.

Figure 5.- Three-degree-of-freedom longitudinal frequency responses neglecting effect of velocity derivatives for three values of trim α. These responses are based on standard sea-level conditions at $M = 1.6$ with $x_{sm} = 0.294\bar{c}$.

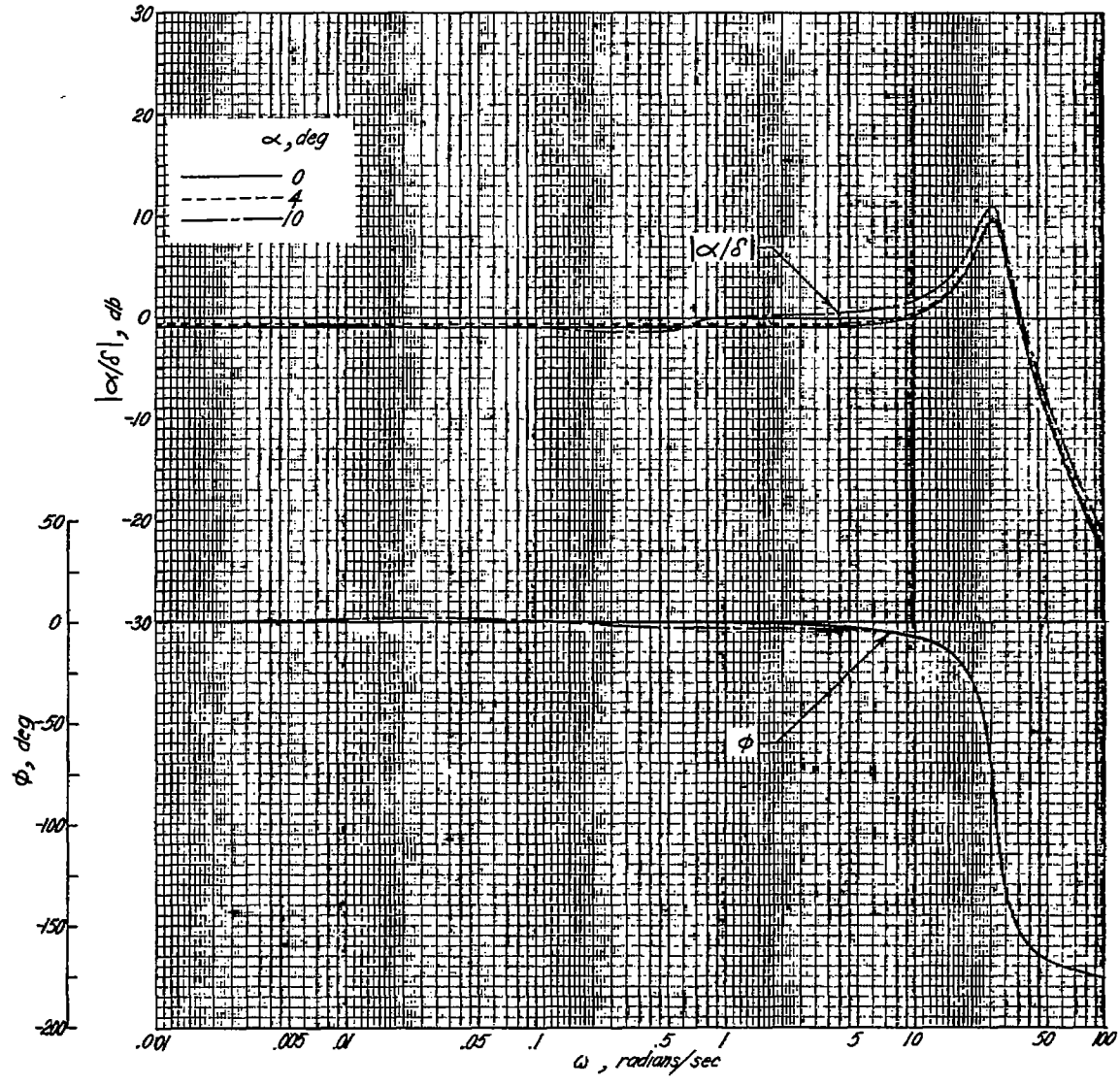

(b) α/δ.

Figure 5.- Continued.

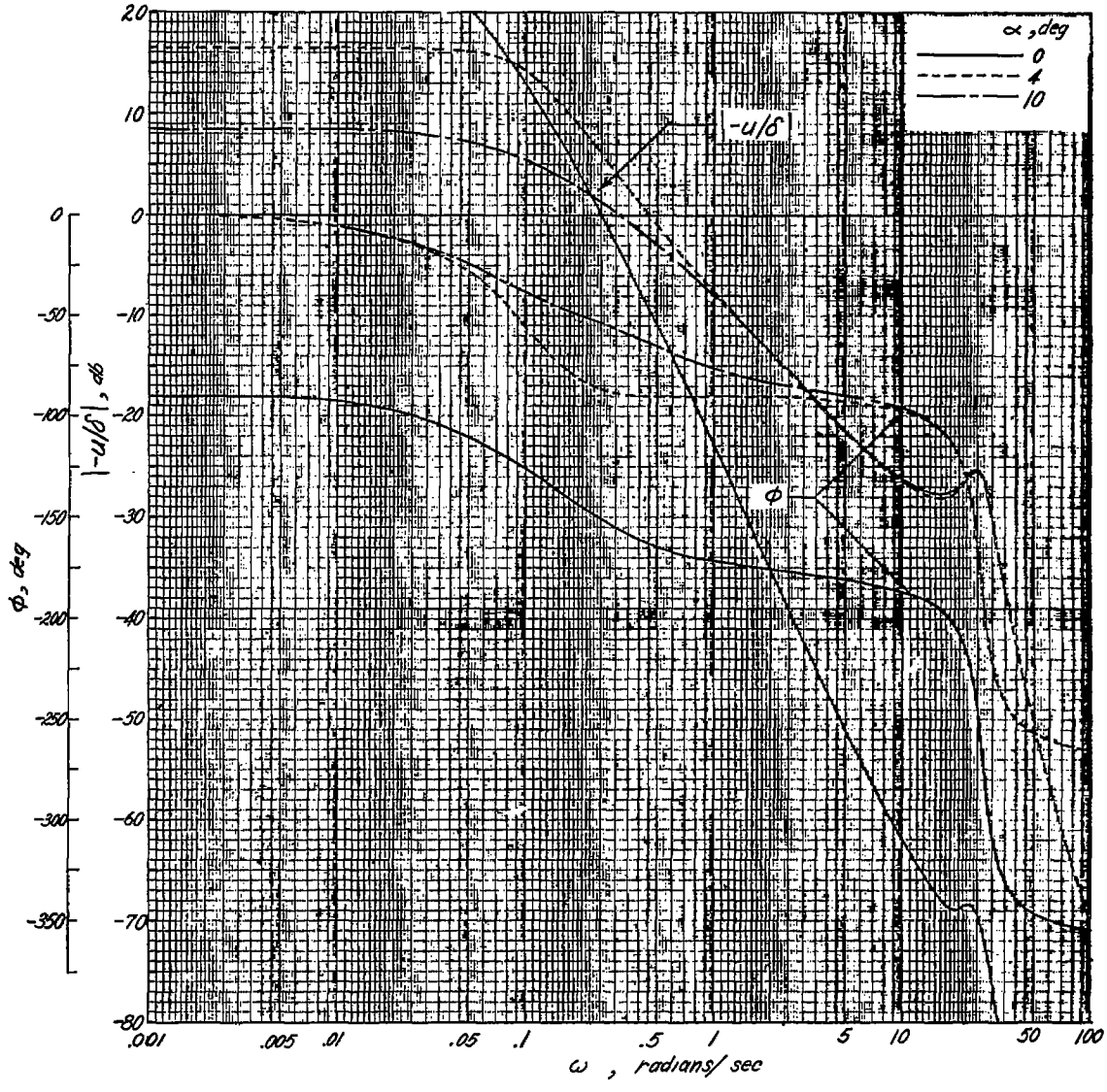

(c) $-u/\delta$.

Figure 5.- Continued.

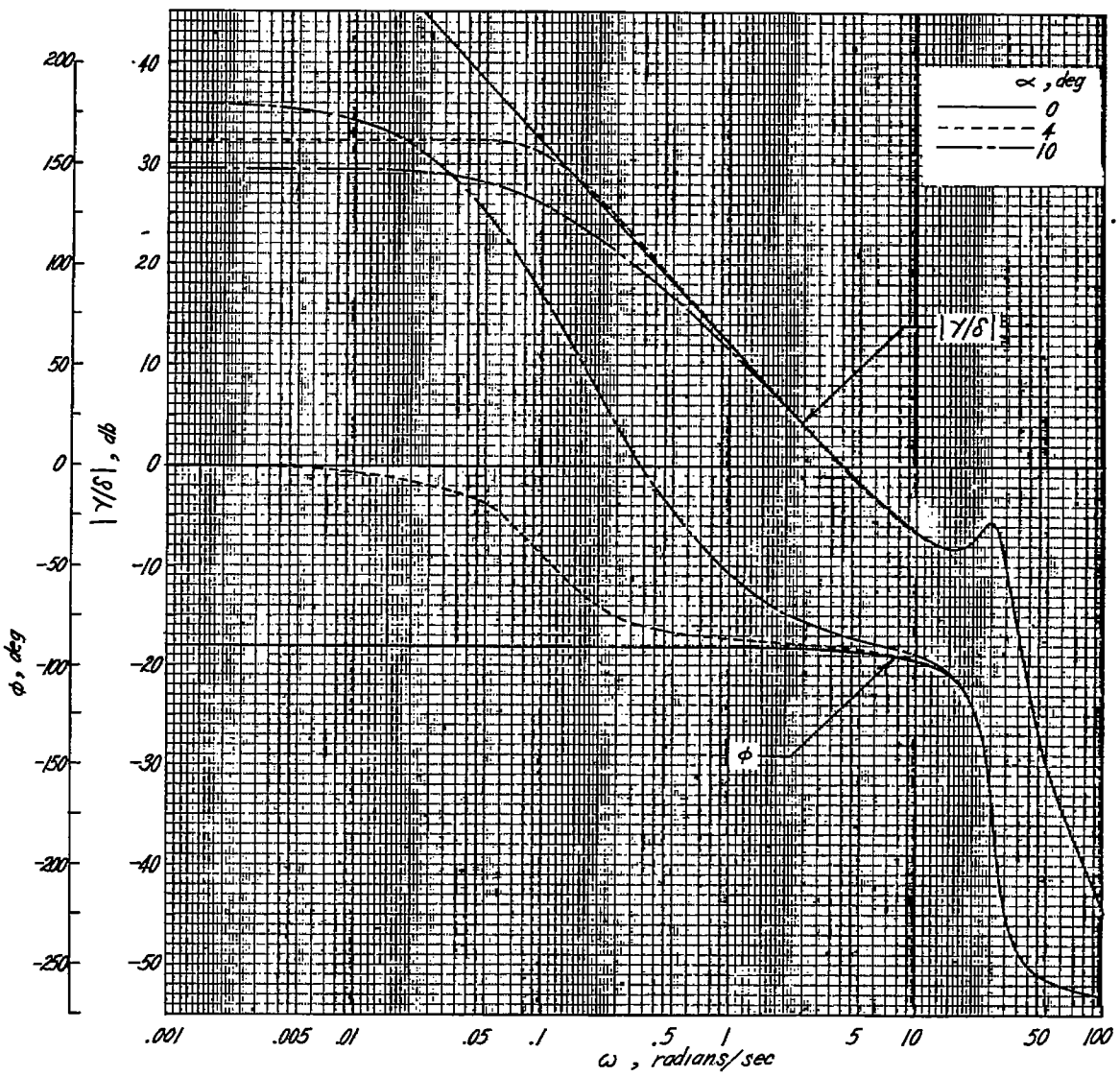

(d) γ/δ.

Figure 5.- Concluded.